Journal of Solid State Chemistry 182 (2009) 3049–3054

Contents lists available at ScienceDirect

Journal of Solid State Chemistry

journal homepage: www.elsevier.com/locate/jssc

Formation of helix-containing rods in a hybrid inorganic–organic material

Zhanhui Yuan [a], William Clegg [a,*], Martin P. Attfield [b,*]

[a] School of Chemistry, Newcastle University, Newcastle upon Tyne NE1 7RU, UK
[b] Centre for Nanoporous Materials, School of Chemistry, University of Manchester, Brunswick Street, Manchester M13 9PL, UK

ARTICLE INFO

Article history:
Received 9 June 2009
Received in revised form
13 August 2009
Accepted 22 August 2009
Available online 28 August 2009

Keywords:
Aluminum
Diphosphonate
Helical structures
Solvothermal synthesis
Hybrid inorganic–organic
Octahedral

ABSTRACT

The novel aluminum ethylenediphosphonate fluoride, $[HN(CH_2CH_2NH_3)_3][Al_2(O_3PCH_2CH_2PO_3)_2F_2]\cdot H_2O$ (**1**) (monoclinic, $P2_1/n$, $a=12.145(4)$ Å, $b=9.265(3)$ Å, $c=20.422(6)$ Å, $\beta=104.952(4)^\circ$, $Z=3$, $R_1=0.092$, $wR_2=0.196$) has been synthesized by solvothermal methods in the presence of tris(2-aminoethyl)amine and its structure determined using single microcrystal X-ray diffraction data. Compound **1** is a one-dimensional extended chain structure composed of well-separated anionic $[Al_2(O_3PCH_2CH_2PO_3)_2F_2]^{4-}$ rods containing helical chains of corner-shared *cis*-AlO_4F_2 octahedra at their core. The charge-compensating tris(2-aminoethyl)ammonium cations separate the anionic $[Al_2(O_3PCH_2CH_2PO_3)_2F_2]^{4-}$ rods that contain either left- or right-handed helical chains. The incorporation of the organic components into this hybrid material has aided the adoption of one-dimensionality by the compound and defined the pitch of the helical AlO_4F chain.

1. Introduction

One-dimensional compounds are of considerable interest because of the fascinating properties that are inherent with their structural anisotropy [1,2]. These properties may include anisotropic electronic conductivity, superconductivity, charge density waves, low-dimensional magnetism or quantum confinement effects [3–7]. It is necessary for the one-dimensional chains in these materials to be isolated to allow truly anisotropic properties to be displayed.

One particular chain structure whose formation is much sought is the helix. This is due in part to the inherent chirality of a helix that may introduce important electric and optical properties into a solid-state structure [8,9]. One of the simplest helical chains that exist consists of metal-centered octahedra with the general formula MX5 and contains homonuclear octahedra that each share two vertices with two adjacent octahedra [10]. Such helices are found to occur in structures where they are directly linked into framework structures, for example, $(C_4H_9NH_3)_2[MFZn_2(HPO_3)_4]$ (NTHU-5) ($M=Al^{3+}$, Ga^{3+}, Fe^{3+}) [11] and $MIn(OH)PO_4$ ($M=NH_4^+$, K^+, Rb^+) [12–15] both containing helical chains of vertex-sharing metal-centered octahedra, or structures that contain one-dimensional helical chains of octahedra separated by metal cations only, for instance, $SrFeF_5$ [16]. However, there are relatively few of these materials that contain well-separated helical MX_5 chains of homonuclear metal-centered octahedra. Formation of well-separated helical chains would allow for the possibility of the properties associated with low dimensionality and those of a helical chain structure to be combined in one periodic array of helices.

The field of hybrid inorganic–organic materials has burgeoned over the past decade with a plethora of new materials with a variety of properties having been reported [17,18]. The formation of such materials presents a possible approach to produce one-dimensional compounds, because the inclusion of an organic component as a structural element of the one-dimensional chain or as a structure-directing agent allows the possibility for isolating extended chain structures, increasing and determining the separation and relative spatial arrangement between the extended chains, and allowing subtle modifications to the chain structure. Such an approach has produced many well-separated one-dimensional chain structures [19–21]. During the course of our program to investigate the structural chemistry of group 13 metal diphosphonates synthesized from a hydrofluoric acid/pyridine solvent system, this versatile approach has led to the discovery of several one-dimensional aluminum diphosphonate chain structures. We have previously reported the synthesis of materials containing separated AlO_4F chains in which the two fluorine vertices of each octahedron are *trans* to each other to form a chain of octahedra in which the central Al atoms are linearly arranged [22], or in which the two fluorine vertices of alternate octahedra are arranged *cis* and *trans* relative to each other along the sequence of AlO_4F octahedra, so forming a chain in which the central Al atoms lie along a zigzag line [23]. These two

* Corresponding authors. Fax: +44 191 222 6929 (William Clegg);
fax: +44 161 275 4598 (M.P. Attfield).
E-mail addresses: w.clegg@ncl.ac.uk (W. Clegg), m.attfield@manchester.ac.uk (M.P. Attfield).

0022-4596/$ - see front matter © 2009 Elsevier Inc. All rights reserved.
doi:10.1016/j.jssc.2009.08.021

chain structures are hybrid analogs of those found in the minerals Tancoite and Laueite, respectively [24,25].

Here we report the hybrid inorganic–organic compound, $(H_4tren)^{4+}[Al_2(O_3PCH_2CH_2PO_3)_2F_2]^{4-}\cdot H_2O$ [tren=$N(CH_2CH_2NH_2)_3$] **1**, the first amine-containing aluminum ethylenediphosphonate fluoride that contains well-separated one-dimensional helical chains of *cis* vertex-sharing homonuclear aluminum-centered octahedra as the main building constituent and whose helical pitch is determined by the diphosphonate linker. The racemic structure contains both left- and right-handed helical chains.

2. Experimental section

2.1. Synthesis and initial characterization

The reagents used in the synthesis of **1** were $Al_2(SO_4)_3\cdot 18H_2O$ (Alfa Aesar), 1,2-ethylenediphosphonic acid (Lancaster), HF (48 wt% in H_2O, Aldrich), pyridine (Aldrich), and tris(2-aminoethyl)amine (tren) (Aldrich). All the aforementioned reagents were used without further purification.

A mixture of $Al_2(SO_4)_3\cdot 18H_2O$, 1,2-ethylenediphosphonic acid, pyridine, HF, tren and water, with a molar ratio of 1:3.75:38.2:4.55:9.54:129, was placed in a Teflon-lined stainless steel autoclave, occupying 25% of the volume, and was heated at 150 °C for 57 days under autogenous pressure. The resulting crystalline product was separated by suction filtration, washed with distilled water, and dried under ambient conditions to yield colorless micro-crystals. The powder X-ray diffraction pattern of this product is provided in the Supporting Information and was judged to be monophasic from the excellent agreement between the experimental powder X-ray diffraction pattern and that calculated using the single-crystal structure of the material [26]. Microprobe EDAX analysis on the product showed that the single crystals contained Al and P in the ratio 1:2, and that fluorine was present.

2.2. Magic angle spinning solid-state NMR (MAS SS NMR) measurement

The MAS SS ^{19}F NMR spectrum was collected from **1** using a Varian Unity Inova spectrometer with a 7.05 T Oxford Instruments magnet and using $CFCl_3$ as a reference.

2.3. Thermogravimetric analysis

Thermogravimetric analysis (TGA) data were collected on **1** using a Shimadzu TGA 50 thermogravimetric analyzer with the sample being heated in a platinum crucible under nitrogen from room temperature to 800 °C at a heating rate of 10 °C min^{-1}.

2.4. Single-crystal X-ray diffraction

Single-crystal X-ray data were collected from a tiny colorless, needle microcrystal of **1** mounted on a Bruker SMART CCD diffractometer at the high-flux single-crystal diffraction station 9.8 at CCLRC (now STFC) Daresbury Laboratory Synchrotron Radiation Source, UK. The crystal was non-merohedrally twinned, preventing the merging of equivalent reflections before refinement. The structure was determined by direct methods and refined by full-matrix least squares using the SHELXTL suite of programs [27]. The aluminum and phosphorus atom positions were determined directly from the structure solution, and the carbon, nitrogen, oxygen and fluorine atoms were located subsequently from difference Fourier maps. The atomic displacement parameters of all of the non-hydrogen atoms were refined anisotropically. The organic tren cation is disordered over two orientations, so restraints were applied to the bond lengths and displacement parameters during refinement. All the hydrogen atoms in the cation and anion were positioned geometrically and constrained with a riding model, with their isotropic atomic displacement factors fixed at values of 1.5 times U_{eq} of the carbon or nitrogen atoms to which they were directly connected. The hydrogen atoms of the non-framework water molecule were not located. The crystallographic data and structure refinement parameters, selected bond distances and selected bond angles

Table 1
Crystallographic data and structure refinement parameters for **1**.

Formula	$C_{10}H_{32}Al_2F_2N_4O_{13}P_4$
Formula weight	632.24
Crystal size (mm)	0.04 × 0.02 × 0.01
Temperature (K)	120(2)
Wavelength (Å)	0.6898 (synchrotron)
Crystal system	Monoclinic
Space group	$P2_1/n$
a (Å)	12.145(4)
b (Å)	9.265(3)
c (Å)	20.422(6)
β (deg)	104.952(4)
V (Å^3)	2220.1(12)
Z	4
D_c (g cm^{-3})	1.891
μ (mm^{-1})	0.511
$2\theta_{min}-2\theta_{max}$ (deg)	4.34–48.08
$F(000)$	1312
Data/restraints/parameters	14425/333/413
R_1 [$I>2\sigma(I)$], R_1 (all data)[a]	0.092, 0.160
wR_2 [$I>2\sigma(I)$], wR_2 (all data)[b]	0.196, 0.224
S on F^2	1.056
Electron density min/max (e Å^{-3})	−0.64/0.66

[a] $R_1=\sum||F_o|-|F_c||/\sum|F_o|$.
[b] $wR_2=\sum[w(F_o^2-F_c^2)^2]/\sum[w(F_o^2)^2]^{1/2}$ with $w=1/[\sigma^2(F_o^2)+(aP)^2+bP]$, $P=[2F_c^2+\mathrm{Max}(F_o^2,0)]/3$, where $a=0.0668$ and $b=10.6604$.

Table 2
Selected bond distances (Å) for **1**.

Al1–F1	1.833(3)	Al1–F2	1.829(3)
Al1–O3	1.874(4)	Al1–O4	1.912(4)
Al1–O5[a]	1.872(7)	Al1–O10[a]	1.861(4)
Al2–F1	1.859(3)	Al2–F2[b]	1.849(3)
Al2–O1	1.868(4)	Al2–O2	1.889(4)
Al2–O8	1.877(4)	Al2–O9	1.866(4)
P1–O3	1.518(4)	P1–O9	1.531(4)
P1–O11	1.523(4)	P1–C4	1.795(6)
P2–O7	1.539(4)	P2–O8	1.513(4)
P2–O10	1.537(4)	P2–C3	1.778(5)
P3–O2	1.500(4)	P3–O4	1.526(4)
P3–O12	1.559(4)	P3–C1	1.808(6)
P4–O1	1.539(4)	P4–O5	1.522(4)
P4–O6	1.520(6)	P4–C2	1.815(6)
C1–C3[b]	1.507(7)	C2–C4[c]	1.524(7)
N1–C5	1.455(13)	N1–C7	1.481(13)
N1–C9	1.426(13)	N2–C6	1.465(13)
N3–C8	1.445(13)	N4–C10	1.393(12)
C5–C6	1.509(13))	C7–C8	1.510(13)
C9–C10	1.531(13)	N1′–C5′	1.434(12)
N1′–C7′	1.467(11)	N1′–C9′	1.439(11)
N2′–C6′	1.451(12)	N3′–C8′	1.453(11)
N4′–C10′	1.333(12))	C5′–C6′	1.533(11)
C7′–C8′	1.498(12))	C9′–C10′	1.539(12)

Symmetry codes: (a) $-x+5/2$, $y-1/2$, $-z+1/2$; (b) $-x+5/2$, $y+1/2$, $-z+1/2$; and (c) x, $y+1$, z.

Table 3
Selected bond angles (deg) for **1**.

F1–Al1–F2	85.1(1)	F1–Al1–O3	88.6(2)
F1–Al1–O4	92.5(2)	F1–Al1–O5[a]	93.5(2)
F1–Al1–O10[a]	174.4(2)	F2–Al1–O3	92.6(2)
F2–Al1–O4	176.3(2)	F2–Al1–O5[a]	89.1(2)
F2–Al1–O10[a]	92.1(2)	O3–Al1–O4	90.1(2)
O3–Al1–O5[a]	177.5(2)	O3–Al1–O10[a]	86.7(2)
O4–Al1–O5[a]	88.3(2)	O4–Al1–O10[a]	90.6(2)
O5[a]–Al1–O10[a]	91.3(2)	F1–Al2–F2[b]	84.2(1)
F1–Al2–O1	173.3(2)	F1–Al2–O2	87.4(2)
F1–Al2–O8	92.9(2)	F1–Al2–O9	92.3(2)
F2[b]–Al2–O1	91.4(2)	F2[b]–Al2–O2	91.6(2)
F2[b]–Al2–O8	87.9(2)	F2[b]–Al2–O9	175.6(2)
O1–Al2–O2	87.7(2)	O1–Al2–O8	92.0(2)
O1–Al2–O9	92.3(2)	O2–Al2–O8	179.4(2)
O2–Al2–O9	90.8(2)	O8–Al2–O9	89.7(2)
O3–P1–O9	112.0(2)	O3–P1–O11	110.6(2)
O3–P1–C4	106.7(2)	O9–P1–O11	111.5(2)
O9–P1–C4	108.5(2)	O11–P1–C4	107.3(2)
O7–P2–O8	110.5(2)	O7–P2–O10	108.5(2)
O7–P2–C3	109.3(2)	O8–P2–O10	113.8(2)
O8–P2–C3	107.1(2)	O10–P2–C3	107.5(2)
O2–P3–O4	114.5(2)	O2–P3–O12	108.7(2)
O2–P3–C1	107.8(2)	O4–P3–O12	111.2(2)
O4–P3–C1	110.4(2)	O12–P3–C1	103.7(2)
O1–P4–O5	112.3(2)	O1–P4–O6	109.4(2)
O1–P4–C2	106.2(2)	O5–P4–O6	112.3(2)
O5–P4–C2	107.2(3)	O6–P4–C2	109.1(2)
P3–C1-C3[b]	112.1(4)	P4–C2–C4c	116.9(4)
P2–C3–C1[a]	116.8(4)	P1–C4–C2[d]	112.6(4)
C5–N1–C7	114.5(12)	C5–N1–C9	119.1(13)
C7–N1–C9	109.1(13)	N1–C5–C6	117.6(13)
N2–C6–C5	109.7(13)	N1–C7–C8	104.9(13)
N3–C8–C7	111.3(17)	N1–C9–C10	114.4(14)
N4–C10–C9	144.8(14)	C5′–N1′–C7′	115.9(11)
C5′–N1′–C9′	119.7(11)	C7′–N1′–C9′	108.0(9)
N1′–C5′–C6′	112.7(10)	N2′–C6′–C5′	110.5(11)
N1′–C7′–C8′	111.9(11)	N3′–C8′–C7′	122.4(12)
N1′–C9′–C10′	103.7(9)	N4′–C10′–C9′	90.0(10)
Al1–F1–Al2	138.8(2)	Al1–F2–Al2	138.8 (2)
Al2–O1–P4	133.8(2)	Al2–O2–P3	137.9(2)
Al1–O3–P1	138.8(2)	Al1–O4–P3	129.8(2)
Al1–O5–P4[b]	138.4(2)	Al2–O8–P2	138.8(2)
Al2–O9–P1	133.4(2)	Al1–O10–P2[b]	132.3(2)

Symmetry codes: (a) $-x+5/2, y-1/2, -z+1/2$; (b) $-x+5/2, y+1/2, -z+1/2$; (c) $x, y+1, z$; and (d) $x, y-1, z$.

for structure **1** are presented in Tables 1–3, respectively. The asymmetric unit of **1** is shown in Fig. 1.

3. Results and discussion

The crystal structure of $(H_4tren)^{4+}[Al_2(O_3PCH_2CH_2PO_3)_2F_2]^{4-}\cdot H_2O$ [tren=$N(CH_2CH_2NH_2)_3$] **1** is shown in Fig. 2. The extended one-dimensional component of **1** is an anionic $[Al_2(O_3PCH_2CH_2PO_3)_2F_2]^{4-}$ rod. The core of these rods contains a helical AlO_4F chain of corner-sharing AlO_4F_2 octahedra as shown in Fig. 3a. Each AlO_4F_2 octahedron consists of a central aluminum atom coordinated by two fluorine atoms arranged in a *cis* configuration. The assignment of the bridging atoms between aluminum centers as fluorine rather than hydroxide groups is soundly based on the significant improvement in the refinement with this assignment, the satisfactory bond lengths and displacement parameters, and the lack of hydrogen bonding for these atoms. Additionally, both microprobe EDAX and solid-state NMR data for crystals of **1** indicate that fluorine is present. The remaining vertices of the AlO_4F_2 octahedron are occupied by oxygen atoms provided by the diphosphonate groups. Each PO_3 group of the diphosphonate ligand binds two adjacent Al centers together, so each diphosphonate group coordinates to a total of four Al centers in the same helical chain through two different pairs of adjacent Al centers at different points along the helical chain as shown in Fig. 3b. This mode of connection of the diphosphonate ligand to the AlO_4F chain is rare within the chemistry of metal diphosphonates and results in the diphsophonate ligand being aligned parallel to the AlO_4F chain, unlike in $(C_3H_7NH_3)AlF[(HO)O_2PC_2H_4PO_3]$, $(H_3NC_2H_4NH_3)Al(OH)[O_3PC_2H_4PO_3]$, $(NH_4)_2AlF(O_3PCH_2PO_3)$ and $(C_5H_5NH)AlF[O_3PCH_2PO_2(OH)]\cdot 0.48H_2O$ where the diphosphonate ligands all lie perpendicular to the portion of the AlO_4F chain to which they are attached [22,23]. The remaining unbound unprotonated oxygen atom of each PO_3 group is directed away from the anionic rod into the inter-rod region. The helical chains of AlO_4F_2 octahedra are surrounded and externally supported by the diphosphonate groups, with both components combining to form the anionic rods of structure **1** running parallel to the *b* axis as shown in Fig. 3b. The average Al–O and Al–F bond distances of 1.877 and 1.843 Å, respectively, agree well with those reported in other aluminum diphosphonate fluorides [22,23]. The tetrahedral PO_3C units display average P–O distances of 1.527 Å and P–C distances of 1.799 Å, values typically found in other metal diphosphonates [28,29]. The ^{19}F SS NMR spectrum of **1** is shown in Fig. 4 and shows one resonance centered at δ −143 ppm. The two crystallographically independent F atoms have essentially identical bond lengths and angles (see Tables 2 and 3, respectively) and hence, presumably, indistinguishable chemical shifts. The chemical shift value of the resonance is typical of those observed in other aluminum diphosphonate fluorides [22,30–32].

The complete structure of **1** viewed along the *b* axis is shown in Fig. 2. The rods are ordered in an approximately hexagonal close-packed arrangement when viewed along their length as seen in Fig. 2. Each rod contains only one chirality of helix, and left- and right-handed helices are arranged alternately in adjacent rows, these rows being oriented parallel to the [101] direction. The anionic $[Al_2(O_3PCH_2CH_2PO_3)_2F_2]^{4-}$ rods are well separated by the $(H_4tren)^{4+}$cations and water molecules located within the interstices. The $(H_4tren)^{4+}$cations adopt a planar configuration and are disordered over two orientations in the inter-rod spaces as shown in Figs. 1 and 2. The two orientations are present at 44.0(5)% and 56.0(5)% occupancy. The atom O13 was assigned as a neutral water molecule in the structure on the basis of appropriate hydrogen bonding contact distances. The anionic rods, and inter-rod $(H_4tren)^{4+}$cations and water molecules, are linked together extensively by hydrogen bonding involving the N–H groups of the cations as donors, the unbound unprotonated oxygen atoms of the PO_3 groups as acceptors, and water molecules acting in both capacities. The range of N donor to O (PO_3, H_2O group) acceptor hydrogen-bonding distances are 2.56(3)–3.17(1) Å with a donor –H$\cdots$ acceptor angular range of 121–172° (see Supporting Information). These distances and angles indicate the hydrogen bonds are of moderate strength and mostly electrostatic in character [33]. The minimum interchain Al$\cdots$Al separation in **1** is 6.932 Å, significantly larger than M$\cdots$M distances in other structures that contain similar separated one-dimensional helical chains of MX_5 octahedra, for instance $SrFeF_5$ (minimum interchain Fe$\cdots$Fe separation 5.044 Å) [16] or $BaFeF_5$ (minimum interchain Fe$\cdots$Fe separation 5.208 Å) [34].

The thermogravimetric trace for compound **1** is shown in Fig. 5 and contains two distinct mass losses: a 2.7% mass loss from 100 to 290 °C due to water removal (calculated 2.8%) and a 19.6% mass loss from 290 to 630 °C due to loss of the fluorine atoms (calculated 6.0%) and incomplete decomposition of the tren molecules (calculated 23.1%) and ethylene groups of diphosphonate units (calculated 8.2%) to yield an amorphous material.

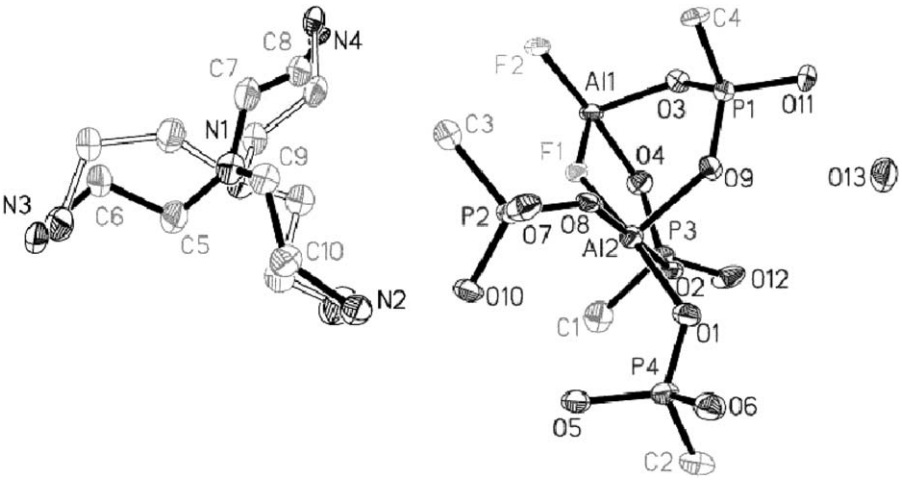

Fig. 1. The asymmetric unit of **1** showing displacement ellipsoids at the 50% probability level. H atoms are omitted. The two orientations of the $(H_4tren)^+$cation are indicated by open and filled bonds.

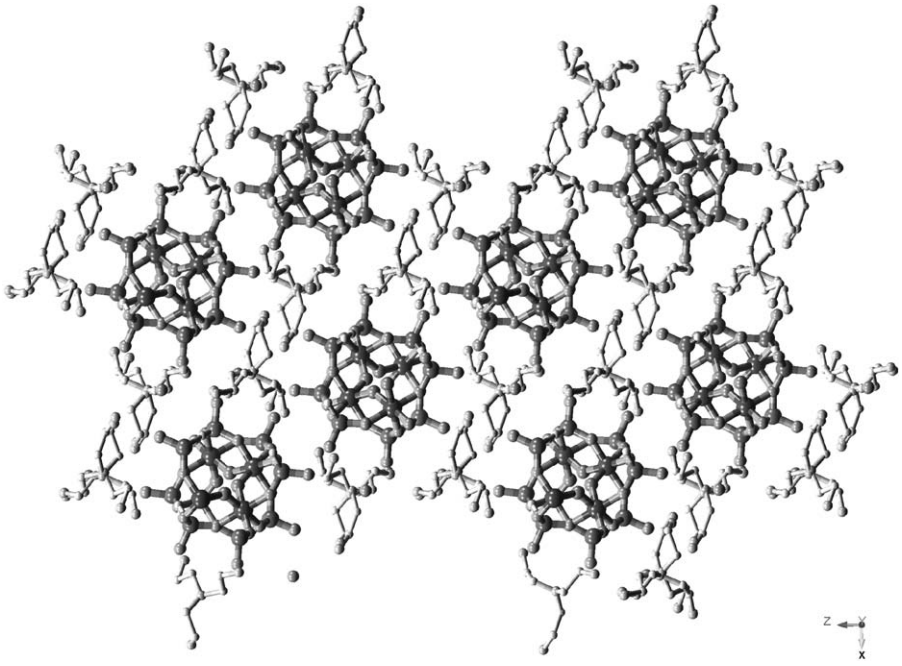

Fig. 2. A ball-and-stick presentation of the structure of **1** viewed down the *b* axis. The water molecule and each of the orientations of the $(H_4tren)^{4+}$cation are shown at the bottom of the figure for clarity. The atoms decrease in size and become lighter in the order: Al, P, F, O, N, C. All H atoms have been omitted.

The use of both organic components in the hybrid material **1** has influenced significantly the crystal structure adopted in several ways. The incorporation of a large structure-directing $(H_4tren)^{4+}$cation in the synthesis mixture helps to form a one-dimensional structure, as the large size of the cation makes it less likely for a three-dimensional framework structure to form around such a bulky cation. The diphosphonate group helps to favor the formation of a one-dimensional structure because the reduction in the number of possible bridging oxygen atoms of the PO_3C group, compared to a phosphate PO_4 group, prevents the helical chains from being directly linked as is observed in MIn(OH)PO_4 (M=NH_4^+, K^+, Rb^+) [12–15], in which structurally similar helical chains to those found in **1** are directly bound together by the phosphate groups. The most significant influence the organic component in the hybrid material **1** has had on the final structure is the determination of the helical pitch of the AlO_4F chains.

The length of the alkyl linker chain of the diphosphonate group in conjunction with flexibility of the chains of octahedra determine the helical pitch of the AlO_4F chains. The helical pitch of the AlO_4F chains in this material is unlikely to be modified significantly through varying the Al–F–Al bond angle as these angles are held relatively firmly at about 140° by the CPO_3 groups that act as rigid braces between adjacent AlO_4F_2 octahedra, with little deviation in the internal O–P–O angles (range of O–P–O bond angles involving oxygen atoms bound to aluminum 112.0–114.5°). However, it should be possible to vary the helical pitch by a torsional motion of the AlO_4F_2 octahedra about the Al–F–Al links

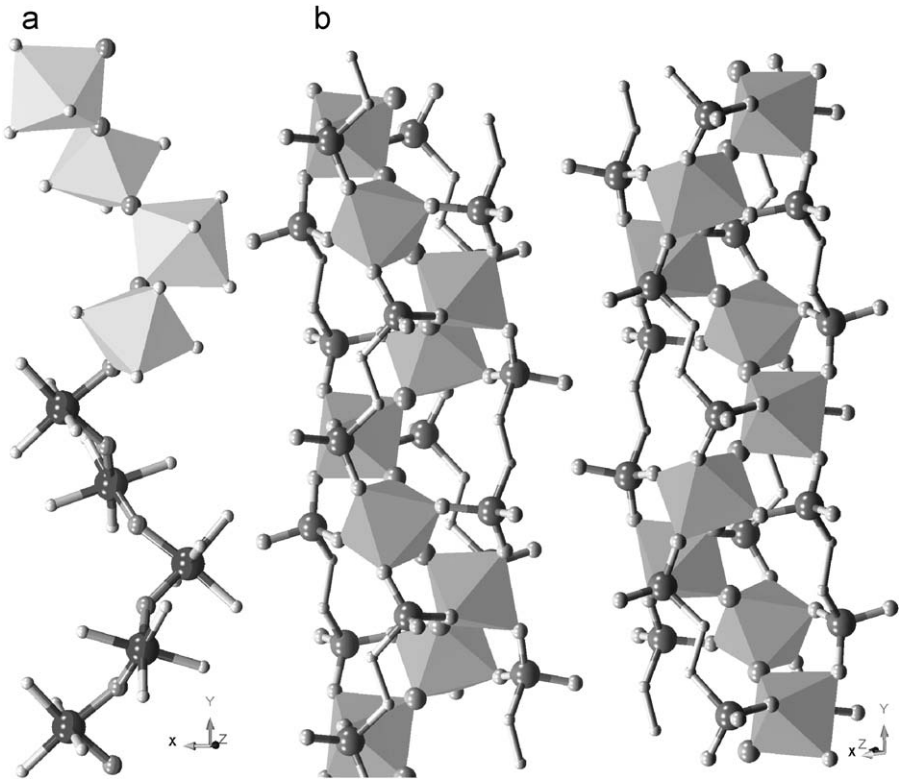

Fig. 3. (a) A polyhedral/ball-and-stick representation of a helical chain of corner-shared *cis*-AlO_4F_2 octahedra that forms the core of the $[Al_2(O_3PCH_2CH_2PO_3)_2F_2]^{4-}_{\infty}$ anionic rods. The atoms decrease in size and become lighter in the order: Al, F, O. (b) A polyhedral/ball-and-stick representation of a pair of $[Al_2(O_3PCH_2CH_2PO_3)_2F_2]^{4-}_{\infty}$ anionic rods each containing a helical chain of corner-shared *cis*-AlO_4F_2 octahedra of opposite handedness. The AlO_4F_2 octahedra are represented as polyhedra and the atoms decrease in size and become lighter in the order: P, F, O, C. All H atoms have been omitted for clarity.

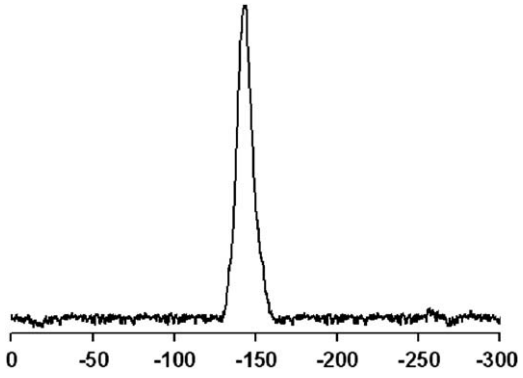

Fig. 4. The ^{19}F MAS SSNMR spectrum of **1**.

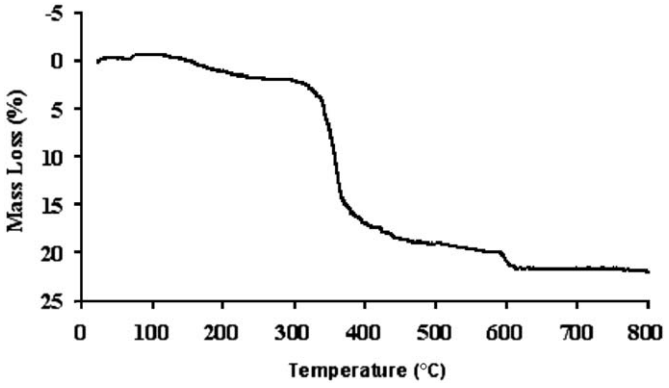

Fig. 5. The thermogravimetric trace of compound **1**.

running along the core of the AlO_4F chains. The torsional motion involves the opposite rotation of adjacent AlO_4F octahedra about the Al–F–Al links and is significantly more likely to occur as it will involve modification of the more flexible P–O–Al angles only (angular range 129.8–138.8°). This type of torsional motion is significant in porous aluminum terephthalates where rotation angles up to 20.3° between consecutive octahedra occur within the *trans* vertex-sharing chains of $AlO_4(OH)_2$ octahedra [35]. Such torsional motion may then accommodate modification of the helical pitch in different structures containing the AlO_4F chain through control of the length of the supporting strut that connects the turns of the helix. The helical pitch in **1** is 9.265 Å as dictated by the length of the supporting ethylenediphosphonate struts. In $(C_4H_9NH_3)_2[AlFZn_2(HPO_3)_4]$ (NTHU-5), which contains an identical helical chain of *cis* vertex-sharing AlO_4F_2 octahedra, the helical pitch is 9.835 Å [11], which is determined by the length and periodicity of the zinc phosphite extended chain that acts as the supporting strut in this structure. Combination of flexibility in the helical chain of octahedra and the supporting strut length may enable further control over the helical pitch by replacing the ethylenediphosphonate groups in this structure with diphosphonate groups containing different sized organic groups, for instance ethene-1,2-diylbisphosphonate, ethyne-1,2-diylbisphosphonate, methylenediphosphonate or propylendiphosphonate. However, the conformation that these diphosphonic acids would have to adopt to be incorporated into the $[Al_2(O_3PRPO_3)_2F_2]^{4-}_{\infty}$ anions will also influence whether the anion can be formed.

The reasons for the formation in **1** of chains of AlO_4F_2 octahedra connected by two fluorine vertices that are *cis* to each other on the AlO_4F_2 octahedra, as opposed to *trans* [22], or a combination of *cis* and *trans* on alternate AlO_4F_2 octahedra [23], are not immediately obvious. The fact that ethylenediphosphonate groups can form one-dimensional $[AlF(O_3PRPO_3)]^{2-}_{\infty}$ chains in which the two fluorine vertices are either *cis* or *trans* on all the AlO_4F_2 octahedra suggests that it is not the diphosphonate group that governs the particular arrangement adopted. It seems likelier that other effects such as the synthesis gel composition, reaction conditions, or the form of the structure-directing agent determine the particular configuration of the AlO_4F chain in the resultant material.

In conclusion, we have isolated compounds containing separated hybrid one-dimensional extended components that contain all three varieties of AlO_4F chain in which the two fluorine vertices of each octahedron are either all *trans*, all *cis* or are arranged *cis* and *trans* relative to each on alternate AlO_4F_2 octahedra. The compound presented in this work contains a periodic array of well-separated anionic rods containing helical AlO_4F chains at their core. The incorporation of the organic components into this hybrid material has aided the formation of a well-separated one-dimensional structure in which a specific structural aspect, the helical pitch, within the resultant material has been determined by the structure of the organic component. This indicates the potential of using both inorganic and organic components to form periodic arrays of isolated one-dimensional components with particular structural features.

Supporting information

The experimental and calculated profile powder X-ray diffraction pattern of 1. Crystallographic data (excluding structure factors) for the structure 1 reported in this paper has been deposited with the Cambridge Crystallographic Data Centre as supplementary publication no. CCDC 294832. Copies of the data can be obtained free of charge on application to CCDC, 12 Union Road, Cambridge CB2 1EZ, UK (fax: +44 1223 336 033; deposit@ccdc.cam.ac.uk).

Acknowledgments

The authors thank Dr. D. Apperley of the EPSRC Solid State NMR Service, University of Durham, UK for collection of the SS MAS NMR data, the EPSRC National Crystallography Service synchrotron component at Station 9.8, Daresbury Laboratory, for the single-crystal X-ray data, and the Chemical and Materials Analysis Service, Newcastle University, for collection of the microprobe EDAX and TGA data. MPA thanks the Royal Society for provision of a University Research Fellowship, and ZY thanks ORS and EPSRC for financial support.

Appendix A. Supplementary material

Supplementary data associated with this article can be found in the online version at 10.1016/j.jssc.2009.08.021.

References

[1] P. Monceau (Ed.), Electronic Properties of Inorganic Quasi-One-Dimensional Compounds, Physics and Chemistry of Materials with Low-dimensional Structures Series B, Parts 1 and 2, D. Reidel, Dordrecht, 1985.
[2] J. Rouxel (Ed.), Crystal Chemistry and Properties of Materials with Quasi-One-Dimensional Structures, Physics and Chemistry of Materials with Low-dimensional Structures Series B, D. Reidel, Dordrecht, 1986;
C.H. Lin, S.L. Wang, K.H. Lii, J. Am. Chem. Soc. 123 (2001) 4649–4650.
[3] K. Carneiro, in: P. Monceau (Ed.), Electronic Properties of Inorganic Quasi-One-Dimensional Compounds, Physics and Chemistry of Materials with Low-dimensional Structures Series B Parts 2, D. Reidel, Dordrecht, 1985, pp. 1–68.
[4] W. Biberacher, H. Schwenk, Solid State Commun. 33 (1980) 385–387.
[5] J.A. Wilson, Phys. Rev. B 19 (1979) 6456–6468.
[6] J.E.L. Waldron, M.A. Green, D.A. Neumann, J. Am. Chem. Soc. (2001) 5833–5834.
[7] X. Huang, J. Li, Y. Zhang, A. Mascarenhas, J. Am. Chem. Soc. (2003) 7049–7055.
[8] P.A. Maggard, A.L. Kopf, C.L. Stern, K.R. Poeppelmeier, Cryst. Eng. Comm. 6 (2004) 451–457.
[9] P.S. Halasyamani, K.R. Poeppelmeier, Chem. Mater. 10 (1998) 2753–2769.
[10] A.F. Wells, Structural Inorganic Chemistry, fifth ed., Oxford University Press, New York, 1984.
[11] Y.L. Lai, K.H. Lii, S.L. Wang, J. Am. Chem. Soc. 129 (2007) 5350–5351.
[12] A.A. Filaretov, M.G. Zhizhin, L.N. Komissarova, V.P. Danilov, V.V. Chernyshev, B.I. Lazoryak, J. Solid State Chem. 166 (2002) 362–368.
[13] S.Y. Mao, M.R. Li, Y.X. Huang, J.X. Mi, H.H. Chen, Z.B. Wei, J.T. Zhao, J. Solid State Chem. 165 (2002) 209–213.
[14] J.A. Hriljac, C.P. Grey, A.K. Cheetham, P.D. VerNooy, C.C. Torardi, J. Solid State Chem. 123 (1996) 243–248.
[15] K.H. Lii, J. Chem. Soc. Dalton Trans. (1996) 815–818.
[16] R. von der Muehll, F. Daut, J. Ravez, J. Solid State Chem. 8 (1973) 206–212.
[17] C. Janiak, Dalton Trans. (2003) 2781–2804 (and references therein).
[18] S.L. James, Chem. Soc. Rev. 32 (2003) 2765–2788 (and references therein).
[19] E. Goreshnik, M. LeBlanc, V. Maisonneuve, J. Solid State Chem. 177 (2004) 4023–4030.
[20] L. Carlucci, G. Ciani, D.M. Proserpio, A. Sironi, Inorg. Chem. (1998) 5941–5943.
[21] B. Morosin, E.J. Graeber, Acta Crystallogr. 23 (1967) 766–770.
[22] H.G. Harvey, S.J. Teat, C.C. Tang, L.M. Cranswick, M.P. Attfield, Inorg. Chem. 42 (2003) 2428–2439.
[23] H.G. Harvey, M.P. Attfield, Solid State Sci. 8 (2006) 404–412.
[24] F.C. Hawthorne, Tschermaks Mineral. Petrogr. Mitt. 31 (1983) 121–135.
[25] P.B. Moore, Am. Min. 50 (1965) 713.
[26] W. Kraus, G. Nolze, PowderCell for Windows, Version 2.4, Germany, 2000.
[27] G.M. Sheldrick, SHELXTL Version 6, Bruker AXS Inc., Madison, Wisconsin, USA, 2001.
[28] M.P. Attfield, H.G. Harvey, S.J. Teat, J. Solid State Chem. 177 (2004) 2951–2960.
[29] H.G. Harvey, A.C. Herve, H.C. Hailes, M.P. Attfield, Chem. Mater. 16 (2004) 3756–3766.
[30] H.G. Harvey, B. Slater, M.P. Attfield, Chem. Eur. J. 10 (2004) 3270–3278.
[31] H.G. Harvey, S.J. Teat, M.P. Attfield, J. Mater. Chem. 10 (2000) 2632–2633.
[32] M.P. Attfield, C. Mendieta-Tan, Z. Yuan, W. Clegg, Solid State Sci. 10 (2008) 1124–1131.
[33] G.A. Jeffrey, An Introduction to Hydrogen Bonding, Oxford University Press, Oxford, 1997.
[34] A. LeBail, A.M. Mercier, Eur. J. Solid State Inorg. Chem. 32 (1995) 15–24.
[35] T. Loiseau, C. Serre, C. Huguenard, G. Fink, F. Taulelle, M. Henry, T. Bataille, G. Ferey, Chem. Eur. J. 10 (2004) 1373–1382.